

A Journal of the Gesellschaft Deutscher Chemiker

# Angewandte Chemie

GDCh

International Edition

www.angewandte.org

## Accepted Article

**Title:** Myxadazoles, Myxobacterium-Derived Isoxazole-Benzimidazole Hybrids with Cardiovascular Activities.

**Authors:** Yuelan Li, Li Zhuo, Xiaobin Li, Yongqiang Zhu, Shuge Wu, Wei Hu, Tao Shen, Yue-Zhong Li, and changsheng wu

This manuscript has been accepted after peer review and appears as an Accepted Article online prior to editing, proofing, and formal publication of the final Version of Record (VoR). This work is currently citable by using the Digital Object Identifier (DOI) given below. The VoR will be published online in Early View as soon as possible and may be different to this Accepted Article as a result of editing. Readers should obtain the VoR from the journal website shown below when it is published to ensure accuracy of information. The authors are responsible for the content of this Accepted Article.

**To be cited as:** *Angew. Chem. Int. Ed.* 10.1002/anie.202106275

**Link to VoR:** <https://doi.org/10.1002/anie.202106275>

## COMMUNICATION

# Myxadazoles, Myxobacterium-Derived Isoxazole-Benzimidazole Hybrids with Cardiovascular Activities

Yuelan Li <sup>†[a]</sup>, Li Zhuo <sup>†[a]</sup>, Xiaobin Li <sup>[b]</sup>, Yongqiang Zhu <sup>[b]</sup>, Shuge Wu <sup>[a]</sup>, Tao Shen <sup>[c]</sup>, Wei Hu <sup>[a]</sup>, Yue-Zhong Li <sup>\*[a]</sup>, and Changsheng Wu <sup>\*[a]</sup>

- [a] Dr. Y.L. Li; <sup>[†]</sup>Dr. L. Zhuo; <sup>[†]</sup>S.G. Wu; Prof. W. Hu; Prof. Y.Z. Li; Prof. C.S. Wu  
State Key Laboratory of Microbial Technology, Institute of Microbial Technology  
Shandong University  
No. 72 Binhai Avenue, Qingdao 266237 (P. R. China)  
E-mail: Prof. C.S. Wu, wuchangsheng@sdu.edu.cn, Tel. (+86) 532 58631539; ORCID ID, 0000-0001-8336-6638; Prof. Y.Z. Li, lilab@sdu.edu.cn; Tel. (+86) 532 58631539; ORCID ID, 0000-0003-1310-0089.
- [b] Dr. X.B. Li; Y.Q. Zhu  
Biology Institute  
Qilu University of Technology (Shandong Academy of Sciences)  
No. 28789 Jingshi Dong Road, Jinan 250103 (P. R. China)
- [c] Dr. T. Shen  
Key Lab of Chemical Biology (MOE), School of Pharmaceutical Sciences  
Shandong University  
No. 44 West Wenhua Road, Jinan 250012 (P. R. China)

<sup>†</sup>These authors contributed equally to this work.

<sup>\*</sup>To whom correspondence should be addressed. wuchangsheng@sdu.edu.cn and lilab@sdu.edu.cn

Supporting information for this article is given via a link at the end of the document.

**Abstract:** *There is a continuous need for novel microbial natural products to fill the drying-up drug development pipeline. Herein, we report myxadazoles from Myxococcus sp. SDU36, a family of novel chimeric small molecules that consist of N-ribityl 5,6-dimethylbenzimidazole and a linear fatty acid chain endowed with an isoxazole ring. The experiments of genome sequencing, gene insertion mutation, isotope labelling, and precursor feeding demonstrated that the fatty acid chain was encoded by a non-canonical PKS/NRPS gene cluster, whereas the origin of N-ribityl 5,6-dimethylbenzimidazole was related to the vitamin B<sub>12</sub> metabolism. The convergence of these two distinct biosynthetic pathways through a C-N coupling led to the unique chemical framework of myxadazoles, which is an unprecedented hybridization mode in the paradigm of natural products. Myxadazoles exhibited potent vasculogenesis promotion effect and moderate antithrombotic activity, underscoring their potential usage for the treatment of cardiovascular diseases.*

Although microbial natural products (NPs) research was once glutted with gloom due to the high rates of rediscovery, genome mining has revealed that microbes harbor a huge reservoir of untapped biosynthetic gene clusters (BGCs), and thus largely revitalized the interest in this field.<sup>[1]</sup> With the cumulative knowledge on microbial biosynthetic logic, we become more and more familiar with several major classes of microbial BGCs,<sup>[2]</sup> like polyketide synthase (PKS),<sup>[3]</sup> non-ribosomal peptide synthetase (NRPS),<sup>[4]</sup> terpene synthase.<sup>[5]</sup> Intriguingly, microbes also evolve versatile interfaces among differential biosynthetic machineries to genetically encode small molecules. The common hybrid biosynthetic systems include but not limited to NRPS-PKS,<sup>[6]</sup> PKS-terpene,<sup>[7]</sup> terpene-alkaloid,<sup>[8]</sup> and terpene-NRPS.<sup>[9]</sup> The improved chemical diversities originated from combinational biosynthesis would be beneficial for microorganisms, in terms of enriching 'chemical language' requisite for molecular interactions or coping with distinct challenges in their native survival environments.<sup>[10]</sup> As we mankind are constantly desperate for novel microbial NPs to deliver new therapeutics for combatting

various diseases,<sup>[11]</sup> it is tempting to explore anomalous combinatorial biosynthetic system(s) to unearth those so-called cryptic "unknown unknowns".<sup>[12]</sup>

The gram-negative myxobacteria have complex social lives and multicellular developmental cycles, involving surface motility, fruiting body formation, sporulation and predatory behavior.<sup>[13]</sup> This branch of life domain is particularly appealing because they have been recognized as one of the foremost producers of specialized metabolites with high chemical complexity and pronounced bioactivities. Myxobacteria are also a prolific source of hybrid biosynthetic logic, such as NRPS-PKS system.<sup>[14]</sup> One of the most prominent examples is epothilone from the myxobacterium *Sorangium cellulosum*, whose semi-synthetic derivatives ixabepilone and utidelone have been approved by FDA (2007) and more recently by SFDA (2021) to treat the breast cancer.<sup>[15]</sup>

As a part of our ongoing efforts to find drug leads from our library of myxobacteria,<sup>[16]</sup> *Myxococcus* sp. SDU36 isolated from the sediment sample of the Dongcuo Lake in Ngari of Tibet (P.R. China) was prioritized for chemical investigation, because it gave a decent number of peaks during the HPLC-based screening. SDU36 was fermented in VY/2 medium (80 L) for seven days, and the metabolites were adsorbed from culture broth using HP-20 resin. The afforded crude extract (8.0 g) was separated by repeated chromatography, and final purification was achieved on a reversed-phase C<sub>18</sub> semi-preparative HPLC, yielding compounds **1** (6.5 mg), **2** (1.8 mg), and **3** (1.2 mg). Their planar structures were established based on intensive analysis of NMR and HRMS data, and the stereochemistry was determined by *J*-based configurational analysis,<sup>[17]</sup> GIAO NMR shift calculations coupled with advanced statistics CP3 analyses,<sup>[18]</sup> quantum topological atoms in molecules (QTAIM) analysis for intramolecular hydrogen bonding interaction,<sup>[19]</sup> as depicted exhaustively in [supporting information](#). Structurally, compounds **1–3** are hybrid NPs consisting of N-ribityl 5,6-dimethylbenzimidazole (DMB) and a fatty acid (FA) chain

## COMMUNICATION

endowed with an isoxazole ring (Figure 1), and we thereby dubbed them as myxadazoles A<sub>1</sub>, A<sub>2</sub>, and B, respectively. Myxadazoles A<sub>1</sub> (1) and A<sub>2</sub> (2) are 7'-epimers (7'S for 1 and 7'R for 2) containing an iso-branched FA. Myxadazole B (3) has the same configurations with 2, but is in possession of an unbranched FA. Only a limited number of NPs containing isoxazole (cycloserins,<sup>[20]</sup> acivicin,<sup>[21]</sup> muscimol,<sup>[22]</sup> and ibotenic acid<sup>[23]</sup>) were reported from actinomycetes and fungi, whereas it was the first time to characterize from the phylum of myxobacteria. What's more striking was that DMB has been only found in vitamin B<sub>12</sub> (VB<sub>12</sub>) besides myxadazoles, highlighting the novelty of the newly identified structures. In addition, although a few isoxazole-benzimidazole hybrids have been artificially synthesized,<sup>[24]</sup> the co-occurrence of isoxazole and DMB was unprecedented in the scope of NPs.

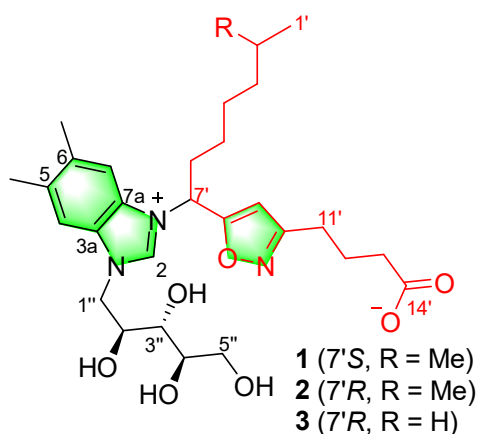


**Figure 1.** Myxadazoles A<sub>1</sub>/A<sub>2</sub> and B (1–3) isolated from *Myxococcus* sp. SDU36.

Besides 1–3, we envisioned that other potential congeners might be produced but escaped from the chromatographic isolation due to the low yield. To verify this assumption, SDU36 crude extract was subjected to MS/MS-based molecular networking analysis,<sup>[25]</sup> wherein structural analogues clustered together (Figure S11). This revealed that the characterized compounds 1–3 were closely related to four additional features at *m/z* 544, 530, 518, and 504 (Figure 2). The comparison of MS<sup>2</sup> fragmentation of these four uncharacterized molecular features (myxadazoles C–F) to those of 1–3, enabled us to conclude that the structural differentiation was located in the FA chain featuring with an isoxazole ring, because the characteristic fragments at *m/z* 281 (*N*-ribityl-DMB) and 147 (DMB) were consistently seen for all six molecular features (Figure S12). Further scrutiny of the fragmentation pattern of all the myxadazoles C–F clarified the major structural variation in the region between isoxazole ring and the terminal carboxyl. There were two less methylenes in myxadazole C (*m/z* 518) than A (*m/z* 546), and a similar structural relationship can be seen between myxadazoles B (*m/z* 532) and D (*m/z* 504). Interestingly, a dehydrogenation occurred in myxadazoles E (*m/z* 544) and F (*m/z* 530) based on the MS/MS comparison with myxadazoles A and B, albeit we did not determine the position and geometry of the double bond.

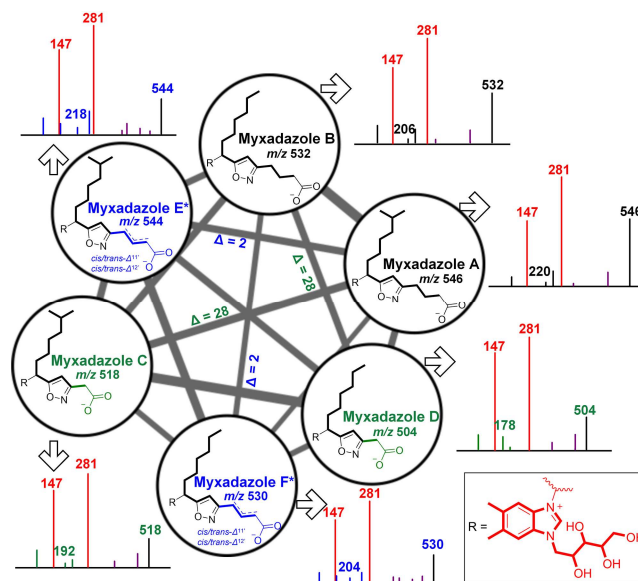


**Figure 2.** Molecular networking of myxadazoles. The key MS<sup>2</sup> fragments used for the determination of myxadazoles C–F was coloured and numbered in accordance with structural variation nearby the terminal carboxyl of lipids. The detailed annotation of the fragmentation referred to Figure S12. \*The position and geometry of the double bond outside the heterocycles in myxadazoles E and F remained undetermined, whereby either  $\Delta^{11,12}$  or  $\Delta^{12,13}$  unsaturation was possible.

To decipher the biosynthetic mechanism of myxadazoles, SDU36 was subjected to genome sequencing by the combination of Nanopore and Illumina technologies. The following antiSMASH analysis of the assembled genome sequence (GenBank accession number: CP077414) gave 28 BGCs.<sup>[26]</sup> Irrespective of the moiety of *N*-ribityl-DMB in myxadazoles, we speculated that the FA part was likely to be assembled by a modular PKS pathway, which was subsequently supported by isotope labeling experiments by feeding SDU36 with [1-<sup>13</sup>C]-acetate (Figure S13). We further reasoned that at least one aminotransferase gene was requisite for the formation of isoxazole ring. After manual analysis of all the 28 BGCs, a non-canonical PKS/NRPS hybrid BGC *mdz* met these constrains. The central biosynthetic elements included two modular PKS genes *mdzE* and *mdzI*, a stand-alone adenylation gene *mdzH*, a seemingly modular NRPS gene *mdzF* integrated with an aminotransferase domain (Figure S14). A BLAST search using the uncommon gene *mdzF* as a probe showed that *mdz* was also contained in 13 other bacterial strains including nine myxobacterial strains. The comparison of the architectural organization of all the gleaned BGCs assisted us to tentatively assign the boundary of *mdz* (Figure S15). This BGC contained nine open reading frames (ORFs) *mdzA*–*mdzI* arranged in the same orientation spanning 21.6 kb on the genome of SDU36 (Figure 3A and Table S7). Co-transcription of *mdzA*–*mdzI* as revealed by RT-PCR experiment suggested they formed a polycistron. To experimentally verify the involvement of *mdz* for myxadazoles production, we selected to genetically disrupt *mdzE* using single crossover recombination (Figure S17). Indeed, myxadazoles A–F were strictly abrogated in the mutant (Figure 4A), corroborating *mdz* was the sought-after BGC.

## COMMUNICATION

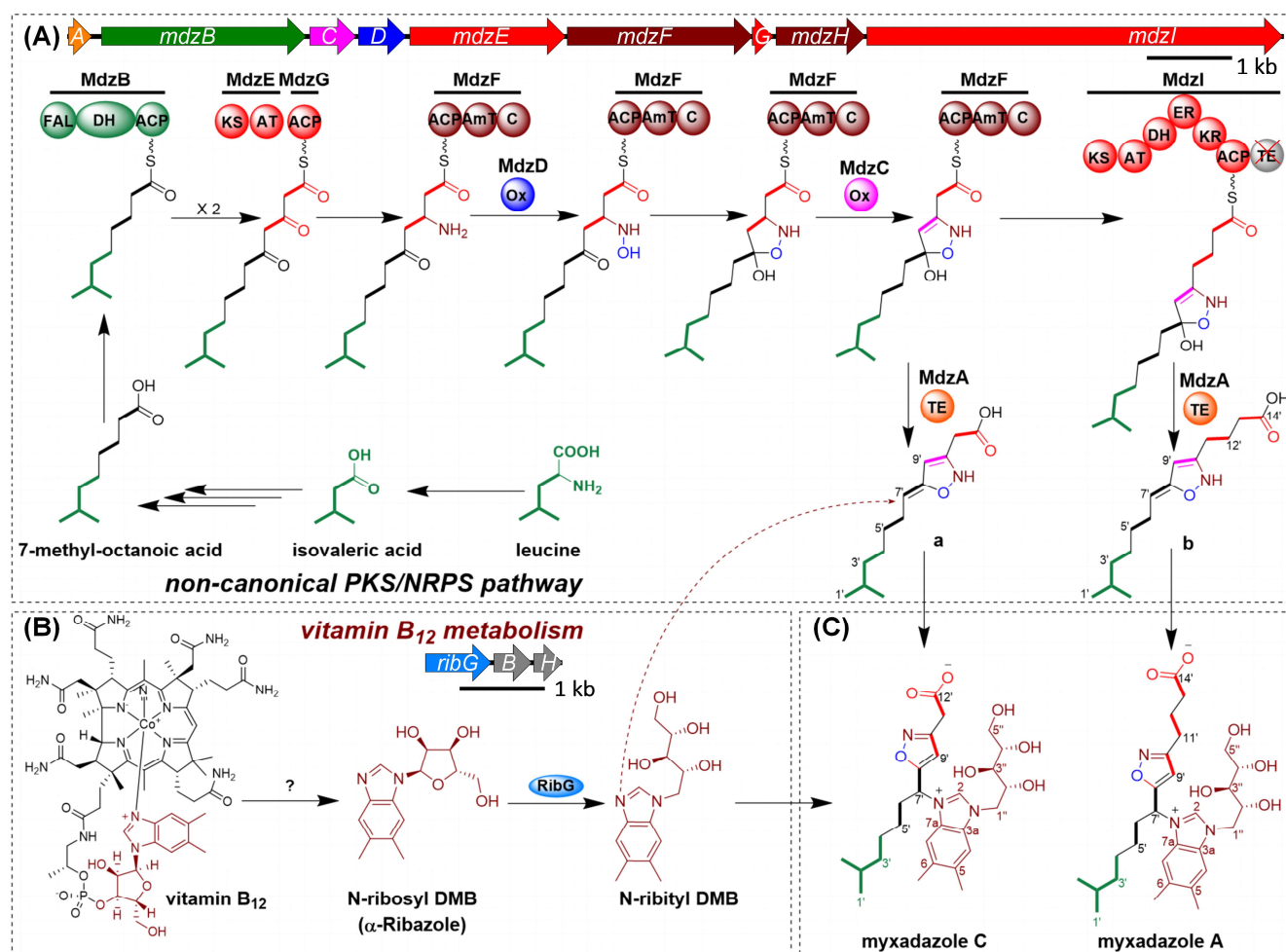


**Figure 3.** Biosynthetic pathway of myxadazoles. **(A)** The non-canonical PKS/NRPS hybrid BGC (*mdz*) directing the biosynthesis of fatty acid. Domain abbreviations: FAL, fatty acid ligase; DH, dehydratase; ACP, acyl carrier protein; KS, ketosynthase; AT, acyltransferase; AmT, aminotransferase; C, condensation; KR, ketoreductase; ER, enoyl reductase; Ox, oxidase; TE, thioesterase. The last putative TE domain in MdzI protein is probably inactive. **(B)** The model for the generation of ribityl DMB from vitamin B<sub>12</sub>. The orphan *rib* BGC contains the *ribG* gene encoding the enzyme that catalyzes the reductive conversion of the ribosyl into ribityl group. **(C)** Representative hybrid products result from the fuse of the alleged two pathways.

Based on the bioinformatic analysis of the central PKS/NRPS genes of *mdz*, we proposed the biosynthetic pathway for myxadazoles as depicted in Figure 3. The assembly line is initiated with the activation of 7-methyl-octanoic acid by the fatty acyl-AMP ligase (FAL) domain in MdzB (In case of myxadazoles B/D/F, octanoic acid should be loaded), followed by two rounds of iterative condensation by the didomain PKS enzyme MdzE, while the growing polyketide chain is tethered on the stand-alone acyl carrier protein (ACP) MdzG. As the iso-odd fatty acids in myxobacteria are originated from leucine,<sup>[27]</sup> SDU36 fed with L-leucine *d*<sub>3</sub> led to the accumulation of isotopic **1** and/or **2** (Figure S18). The priming model was further confirmed by the precursor feeding of isovaleric acid (IVA), which significantly enhanced the production of myxadazole A (Figure S19). After extension by MdzE/MdzG complex, a transamination occurred at the second carbonyl of the nascent polyketidic chain, followed by *N*-hydroxylation catalyzed by the oxidase MdzD. The condensation (C) domain in MdzF probably catalyzes the cyclization of the generated oximes species to yield the isoxazolidine scaffold, since it resides in the heterocyclization sub-branch of phylogenetic tree for C domains of NRPS (Figure S20).<sup>[28]</sup> The isoxazolidine ring is further oxidized into isoxazoline as executed by the FA desaturase MdzC. The cascade reactions including amination, *N*-hydroxylation, heterocyclization, and

desaturation that result in isoxazoline were reminiscent of the recently uncovered biosynthetic logic for ibotenic acid wherein an isoxazole ring is contained.<sup>[29]</sup> Next, the polyketidic chain is further extended with a reduced C<sub>2</sub> unit by the action of MdzI. Because the putative thioesterase (TE) domain at the C terminal of MdzI is hampered due to the deficiency of the critical catalytic triad (Figure S21),<sup>[30]</sup> the mature chain is supposed to be released by MdzA, a discrete type II TE enzyme. It was noteworthy that the single methylene between the terminal carboxyl and isoxazole found in myxadazoles C/D implied that MdzA could act prior to MdzI. The premature release of polyketide chain by MdzA was further supported by the genetic inactivation of *mdzI*, whereby myxadazoles A/B were fully abolished, in stark contrast to the elevated yield of myxadazoles C and D (Figure 4A). Finally, these two released chains might go through a spontaneous dehydration at the hemiacetal, to afford a double bond between C-7' and C-8' in the polyketidic intermediates **a** and **b**.

The unique existence of  $\alpha$ -D-ribosyl-DMB ( $\alpha$ -Ribazole) in VB<sub>12</sub> implied that VB<sub>12</sub> is the source of *N*-ribityl-DMB in myxadazoles. This was reflected by the exogenous addition of 0.1 mM of VB<sub>12</sub> to the producing VY/2 medium, resulting in more than two-fold enhancement of myxadazoles. Similar increasing pattern was also observed for CTT medium poor in VB<sub>12</sub> (Figure

## COMMUNICATION

4B). Taken together of 4-fold lower myxadazoles production in basal CTT than in VY/2, *N*-ribityl-DMB moiety in myxadazoles should be derived from  $\alpha$ -D-ribosyl-DMB of VB<sub>12</sub>. Since  $\alpha$ -D-ribosyl-DMB could be released from VB<sub>12</sub> by non-enzymatic acid hydrolysis *in vitro*,<sup>[31]</sup> it was likely that either enigmatic enzymatic reaction(s) or a decreased pH played a crucial role in the degradation of VB<sub>12</sub>. Next, the cyclic ribosyl-DMB is opened to ribityl-DMB, in the same fashion for the generation of linear ribityl during riboflavin biosynthesis.<sup>[32]</sup> As *mdz* obviously lacks the genes metabolizing VB<sub>12</sub>, we postulated they are located elsewhere on the genome of SDU36. Indeed, bioinformatics analysis identified an operon pertinent to riboflavin, wherein the product of bifunctional gene *ribG* (Table S8) can catalyze the reduction of the ribosyl side chain.<sup>[32]</sup> Furthermore, spectroscopic methods determined the same absolute configuration of the ribityl chain between myxadazole and riboflavin (Table S2 and S3), also suggesting the transformation route depicted in Figure 3B.

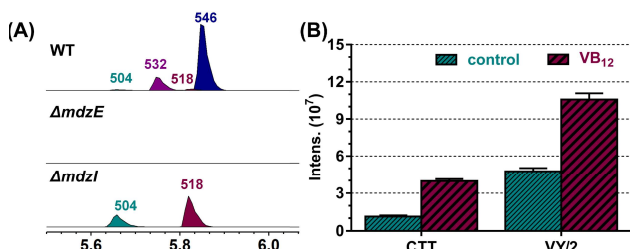


**Figure 4.** (A) Gene disruption of the two central PKS genes *mdzE* and *mdzI* confirmed the correlation of *mdz* with myxadazoles production. (B) Supplementing SDU36 with 0.1 mM of VB<sub>12</sub> grown in media CTT and VY/2 led to three- and two-fold improvements in myxadazoles production, respectively.

We proposed the final convergence of the putative VB<sub>12</sub> metabolic pathway and the non-canonical PKS/NRPS pathway through a C-N coupling leads to the chimeric structure of myxadazoles (Figure 3). A non-stereoselective epoxidation probably occurs at the double  $\Delta^{7,8}$  of intermediates *a/b*. The electron-deficient epoxide species is susceptible to nucleophilic attack by the N-1 atom of benzimidazole, leading to two possible epimers at C-7', followed by a subsequent elimination of one molecule of water to make the isoxazole ring (Figure S22). Versatile C-N coupling reaction<sup>[33]</sup> is probably a more commonplace strategy taken by nature than previously recognized, which merges distinct biosynthetic machineries and thus results in the mixed biosynthesis of a variety of chimeric NPs. Besides myxadazoles, C-N coupling also serves as a port to mediate the heterodimerization of structurally complex terpene-alkaloid conidiogenone B<sup>[34]</sup> and the enediyne-anthraquinone dynemicin A.<sup>[35]</sup>

The isolated myxadazoles A<sub>1</sub>/A<sub>2</sub> and B (1–3) were assayed for the activities of antibacterial (against *Staphylococcus aureus*, *Bacillus subtilis*, *Escherichia coli*, and *Acinetobacter baumannii*), antifungal (against *Candida albicans*), anti-cancer (against liver carcinoma cell line HepG2, breast cancer cell line MCF-7, and hepatocyte cell line HL-7702), antioxidant (DPPH radical-scavenging), and anti-inflammatory (inhibited LPS-induced NO production in adherent cells), whereas no obvious effects were observed. We further evaluated the potential efficacy of myxadazoles on cardiovascular system in zebrafish.<sup>[36]</sup> The model of PTK787-induced intersomitic vessel (ISVs) insufficiency was employed for the promotion of vasculogenesis. The tested compounds at two moderate concentrations (10  $\mu$ M

and 25  $\mu$ M) could markedly rescue the blood vessel loss caused by PTK787 (Figure 5, A & C), whereby the vascular lengths were comparable to those recovered by positive control Danhong injection (DHI, 9  $\mu$ L/mL). In addition, the pathological model of arachidonic acid (AA)-induced thrombosis was used for the evaluation of antithrombotic effects.<sup>[37]</sup> Myxadazoles significantly increased the erythrocytes in the heart of AA-treated zebrafish and decreased the thrombus in caudal vein (Figure 5, B & D). Among them, 1 gave the best therapeutic efficacies of 31.7% and 59.0% at the given two doses, compared with 71.1% obtained by the positive control group of aspirin (ASP, 166  $\mu$ M) (Table S9). Taken together, the non-cytotoxicities, pronounced vasculogenesis, and moderate antithrombotic effects of myxadazoles underscored their potential usage in the treatment of cardiovascular diseases.

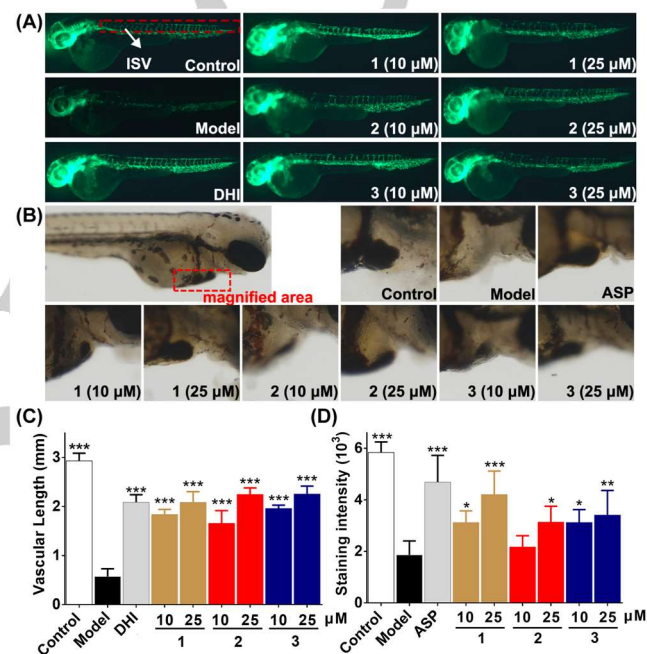


**Figure 5.** Cardiovascular activities test of myxadazoles using zebrafish model. (A) Images of intersomitic vessels (ISVs) in transgenic fluorescent zebrafish [Tg: flil1-EGFP] treated with 0.1% v/v of DMSO (Control), PTK787 along with 0.1% v/v of DMSO (Model), PTK787 along with Danhong injection (DHI, 9  $\mu$ L/mL, positive control), and PTK787 along with two different doses (10  $\mu$ M and 25  $\mu$ M) of compounds 1–3. (B) Images of erythrocytes in the heart of zebrafish treated with 0.1% v/v of DMSO (Control), arachidonic acid (AA) along with 0.1% v/v of DMSO (Model), AA along with aspirin (ASP, 160  $\mu$ M, positive control), and AA along with two different doses (10  $\mu$ M and 25  $\mu$ M) of compounds 1–3. Black spot in the magnified area indicated the staining of erythrocytes in the heart. (C) Quantitative analysis of the length of ISV in zebrafish treated with compounds 1–3. Data represented as mean  $\pm$  SEM, \*\*\*P < 0.001 compared to the model group; (D) Quantitative analysis of the staining intensity of erythrocytes in the heart of zebrafish treated with compounds 1–3 compared to the model group. Data represented as mean  $\pm$  SEM, \*\*\*P < 0.001, \*\*P < 0.01 and \*P < 0.05 compared to the model group.

Cumulatively, with the aid of MS/MS-based molecular networking, we have characterized a family of naturally occurring isoxazole-benzimidazole hybrids that exhibited appreciable cardiovascular activities. The biosynthetic pathway of myxadazoles was probed by bioinformatic analysis, gene insertion mutation, isotope labelling, and precursor feeding. Surprisingly, myxadazoles are originated from the convergence of vitamin B<sub>12</sub> metabolism and a non-canonical PKS/NRPS pathway, which has no precedent examples hitherto. It would be interesting to explore whether the alleged two distinct pathways

## COMMUNICATION

are joined at the metabolomic or genetic level, because this will be of marked value for future multidisciplinary approaches to make a panel of polyketide-alkaloid hybrid (un)natural products. While a growing body of interest has been laid on the excavation of novel microbial NPs, the exploration of the condensation of disparate biosynthetic machineries would be a fruitful approach to find the hidden “unknown unknowns”. Development of versatile discovery pipelines performed in high-throughput manner are desperately needed, because the currently prevailing (meta)genomics-based approaches will miss a considerable amount of undescribed chemistry originated from crosstalk of different BGCs.

## Acknowledgements

We gratefully acknowledge Prof. Dr. Yizhen Yin and Prof. Dr. Longyang Dian (Institute of Microbial Technology, Shandong University), and Dr. Wen-Xuan Wang (Xiangya College of Pharmacy, Central South University) for valuable discussions. This work was financially supported by the National Key Research and Development Programs of China (no. 2019YFA0905700, 2021YFC2101000, 2018YFA0900400, and 2018YFA0901704), the National Natural Science Foundation of China (NSFC) (no. 81973215, 31900042, 31670076, and 31471183), Excellent Youth Program of Shandong Natural Science Foundation (no. ZR2020YQ62, and the Qingdao Postdoctoral Application Research Project (no. 62450070311089).

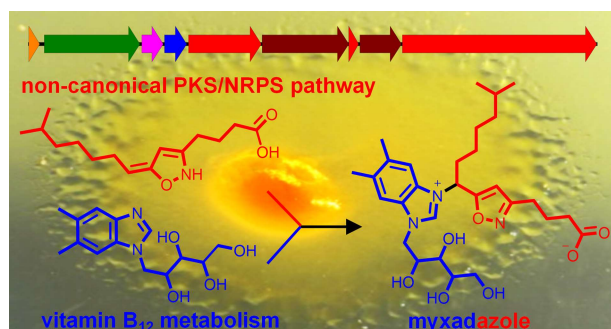
**Keywords:** isoxazole-benzimidazole hybrids • myxadazoles • molecular networking analysis • precursor-directed biosynthesis • cardiovascular activities

## Reference

- [1] A. L. Harvey, R. Edrada-Ebel, R. J. Quinn, *Nat. Rev. Drug Discov.* **2015**, *14*, 111-129.
- [2] a) C. T. Walsh, Y. Tang, *Natural Product Biosynthesis: Chemical Logic and Enzymatic Machinery*, Royal Society of Chemistry, Cambridge, England, **2017**; b) I. Kjærboelling, U. H. Mortensen, T. Vesth, M. R. Andersen, *Fungal Genet. Biol.* **2019**, *130*, 107-121.
- [3] C. P. Ridley, H. Y. Lee, C. Khosla, *PNAS* **2008**, *105*, 4595-4600.
- [4] D. Schwarzer, R. Finking, M. A. Marahiel, *Nat. Prod. Rep.* **2003**, *20*, 275-287.
- [5] D. W. Christianson, *Chem. Rev.* **2017**, *117*, 11570-11648.
- [6] A. Miyanaga, F. Kudo, T. Eguchi, *Nat. Prod. Rep.* **2018**, *35*, 1185-1209.
- [7] a) M. Jiang, Z. Wu, L. Liu, S. Chen, *Org. Biomol. Chem.* **2021**, *19*, 1644-1704; b) L. F. Tietze, H. P. Bell, S. Chandrasekhar, *Angew. Chem. Int. Ed.* **2003**, *42*, 3996-4028.
- [8] a) S. E. O'Connor, J. J. Maresh, *Nat. Prod. Rep.* **2006**, *23*, 532-547; b) Y. Shen, W.-J. Liang, Y.-N. Shi, E. J. Kennelly, D.-K. Zhao, *Nat. Prod. Rep.* **2020**, *37*, 763-796.
- [9] D. A. Yee, T. B. Kakule, W. Cheng, M. Chen, C. T. Y. Chong, Y. Hai, L. F. Hang, Y.-S. Hung, N. Liu, M. Ohashi, I. C. Okorafor, Y. Song, M. Tang, Z. Zhang, Y. Tang, *J. Am. Chem. Soc.* **2020**, *142*, 710-714.
- [10] M. Bae, E. Mevers, G. Pishchany, S. G. Whaley, C. O. Rock, D. R. Andes, C. R. Currie, M. T. Pupo, J. Clardy, *Org. Lett.* **2021**, *23*, 1648-1652.
- [11] A. G. Atanasov, S. B. Zotchev, V. M. Dirsch, I. N. P. S. Taskforce, C. T. Supuran, *Nat. Rev. Drug Discov.* **2021**, *20*, 200-216.
- [12] P. A. Hoskisson, R. F. Seipke, *mBio* **2020**, *11*, e02642-02620.
- [13] J. Muñoz-Dorado, F. J. Marcos-Torres, E. García-Bravo, A. Moraleda-Muñoz, J. Pérez, *Front. Microbiol.* **2016**, *7*, 781-781.
- [14] a) K. J. Weissman, R. Mueller, *Nat. Prod. Rep.* **2010**, *27*, 1276-1295; b) S. C. Wenzel, R. Mueller, *Nat. Prod. Rep.* **2007**, *24*, 1211-1224; c) R. Kaur, A. Kumari, R. Kaur, R. Kaur, *Int. J. Res. Pharm. Sci. (Madurai, India)* **2018**, *9*, 309-313; d) J. Herrmann, A. A. Fayad, R. Muller, *Nat. Prod. Rep.* **2017**, *34*, 135-160.
- [15] a) H. S. Rugo, H. Roche, E. Thomas, H. C. Chung, G. L. Lerzo, I. Vasyutin, A. Patel, L. Vahdat, *Clin. Breast Cancer* **2018**, *18*, 489-497; b) B. Xu, T. Sun, Q. Zhang, P. Zhang, Z. Yuan, Z. Jiang, X. Wang, S. Cui, Y. Teng, X. C. Hu, J. Yang, H. Pan, Z. Tong, H. Li, Q. Yao, Y. Wang, Y. Yin, P. Sun, H. Zheng, J. Cheng, J. Lu, B. Zhang, C. Geng, J. Liu, K. Shen, S. Yu, H. Li, L. Tang, R. Qiu, *Ann. Oncol.* **2021**, *32*, 218-228.
- [16] J.-Q. Hu, J.-J. Wang, Y.-L. Li, L. Zhuo, A. Zhang, H.-Y. Sui, X.-J. Li, T. Shen, Y. Yin, Z.-H. Wu, W. Hu, Y.-Z. Li, C. Wu, *Org. Lett.* **2021**, *23*, 2114-2119.
- [17] G. Bifulco, P. Dambrosio, L. Gomez-Paloma, R. Riccio, *Chem. Rev.* **2007**, *107*, 3744-3779.
- [18] S. G. Smith, J. M. Goodman, *J. Org. Chem.* **2009**, *74*, 4597-4607.
- [19] H. J. Bohórquez, R. J. Boyd, C. F. Matta, *J. Phys. Chem. A* **2011**, *115*, 12991-12997.
- [20] a) M.-L. Svensson, S. Gatenbeck, *Arch. Microbiol.* **1982**, *131*, 129-131; b) T. Kumagai, Y. Koyama, K. Oda, M. Noda, Y. Matoba, M. Sugiyama, *Antimicrob. Agents Chemother.* **2010**, *54*, 1132-1139.
- [21] a) S. J. Gould, S. Ju, *J. Am. Chem. Soc.* **1993**, *114*, 10166-10172; b) S. J. Gould, S. Ju, *J. Am. Chem. Soc.* **1989**, *111*, 2329-2331.
- [22] M. Onda, H. Fukushima, M. Akagawa, *Chem. Pharm. Bull.* **1964**, *12*, 751-751.
- [23] K. Bowden, A. C. Drysdale, G. A. Moge, *Nature* **1965**, *206*, 1359-1360.
- [24] a) A. Masuda, K. Gohda, Y. Iguchi, K. Fujimori, Y. Yamashita, K. Oda, M. Une, N. Teno, *Biorg. Med. Chem.* **2020**, *28*, 115512; b) B. Ashok Kumar, V. Shanmukha Kumar Jagarlapudib, *Russ. J. Gen. Chem.* **2019**, *89*, 2512-2515.
- [25] J. Y. Yang, L. M. Sanchez, C. M. Rath, X. Liu, P. D. Boudreau, N. Bruns, E. Glukhov, A. Wodtke, R. de Felicio, A. Fenner, W. R. Wong, R. G. Linington, L. Zhang, H. M. Debonsi, W. H. Gerwick, P. C. Dorrestein, *J. Nat. Prod.* **2013**, *76*, 1686-1699.
- [26] a) K. Blin, S. Shaw, S. A. Kautsar, M. H. Medema, T. Weber, *Nucleic Acids Res.* **2021**, *49*, D639-D643; b) K. Blin, S. Shaw, K. Steinke, R. Villebro, N. Ziemert, S. Y. Lee, M. H. Medema, T. Weber, *Nucleic Acids Res.* **2019**, *47*, W81-W87.
- [27] H. B. Bode, J. S. Dickschat, R. M. Kroppenstedt, S. Schulz, R. Mueller, *J. Am. Chem. Soc.* **2005**, *127*, 532-533.
- [28] C. Rausch, I. Hoof, T. Weber, W. Wohlleben, D. H. Huson, *BMC Evol. Biol.* **2007**, *7*, 78.
- [29] S. Obermaier, M. Müller, *Angew. Chem. Int. Ed.* **2020**, *59*, 12432-12435.
- [30] J. J. Gehret, L. Gu, W. H. Gerwick, P. Wipf, D. H. Sherman, J. L. Smith, *J. Biol. Chem.* **2011**, *286*, 14445-14454.
- [31] A. Schnellbaecher, D. Binder, S. Bellmaine, A. Zimmer, *Biotechnol. Bioeng.* **2019**, *116*, 1537-1555.
- [32] G. Richter, M. Fischer, C. Krieger, S. Eberhardt, H. Lüttgen, I. Gerstenschläger, A. Bacher, *J. Bacteriol.* **1997**, *179*, 2022-2028.
- [33] a) P. Ruiz-Castillo, S. L. Buchwald, *Chem. Rev.* **2016**, *116*, 12564-12649; b) J. Bariwal, E. Van der Eycken, *Chem. Soc. Rev.* **2013**, *42*, 9283-9303.
- [34] R. T. Hewage, R.-J. Huang, S.-J. Lai, Y.-C. Lien, S.-H. Weng, D. Li, Y.-J. Chen, S.-H. Wu, R.-J. Chein, H.-C. Lin, *Org. Lett.* **2021**, *23*, 1904-1909.
- [35] D. R. Cohen, C. A. Townsend, *Chembiochem* **2020**, *21*, 2137-2142.
- [36] M. Zhang, P. Li, F. Wang, S. Zhang, H. Li, Y. Zhang, X. Wang, K. Liu, X.-B. Li, *Food Funct.* **2021**.
- [37] T. Li, X. Tang, X. Luo, Q. Wang, K. Liu, Y. Zhang, N. J. de Voogd, J. Yang, P. Li, G. Li, *Org. Lett.* **2019**, *21*, 9483-9486.

## COMMUNICATION

## Entry for the Table of Contents



Herein, we report myxadazoles from *Myxococcus* sp. SDU36, a family of novel chimeric small molecules with sound cardiovascular activities. Myxadazoles consist of a N-ribityl 5,6-dimethylbenzimidazole and a fatty acid chain endowed with an isoxazole ring. The fatty acid chain was encoded by a non-canonical PKS/NRPS gene cluster, whereas the N-ribityl 5,6-dimethylbenzimidazole ring was originated from the endogenous vitamin B<sub>12</sub> metabolism pathway. A plausible C-N cross coupling is likely to coordinate the convergence of these two distinct biosynthetic pathways that led to the final construction of unique chemical scaffold of myxadazoles.